Transactions, SMiRT-22
San Francisco, California, USA - August 18-23, 2013
Division I

EVALUATION OF MATERIAL STRESS-STRAIN BEHAVIOR OF PRESSURE TUBES OF HEAVY WATER REACTORS USING FE ANALYSIS OF RING-TENSILE TESTS

M.K. Samal[1], K.S. Balakrishnan[2], V. Bhasin[1], K.K. Vaze[1], S.Anantharaman[2]

[1]Reactor Safety Division, Bhabha Atomic Research Centre, Mumbai-400085, India
[2]Post Irradiation Examination Division, Bhabha Atomic Research Centre, Mumbai-400085, India

ABSTRACT

Determination of transverse mechanical properties from the ring type of specimens directly machined from the nuclear reactor pressure tubes is not straightforward because of the presence of combined membrane as well as bending stresses arising in the loaded condition. In this work, we have performed ring-tensile tests on the un-irradiated ring tensile specimens using two split semi-cylindrical mandrels as the loading device. A 3-D finite element (FE) analysis was performed in order to determine the material true stress-strain curve by comparing experimental load-displacement data with those predicted by FE analysis. We have analyzed the deformation behavior of ring-tension specimens machined from two different types of Zirconium alloy pressure tubes as used in the Indian pressurized heavy water reactors. The effect of geometry of the loading mandrel (i.e., 2-piece vs. 3-piece type of mandrel) on the load-deformation behavior of the test-setup has been studied. It was observed that the values of maximum load as well as the deformation behavior in the post-necking region differ significantly when only the geometry of the loading-mandrel is changed keeping all the other parameters same. However, finite element analysis have been able to correctly predict these variations as it takes into account of the effect of geometry, material properties as well the interaction between the mandrel and the specimen. Hence, the use of finite element method is essential in the inverse analysis procedure where the material properties can be determined from these complex test-setups.

Keywords: Ring-tension test; Finite element analysis; Zirconium alloy; Pressure tube material

INTRODUCTION

Pressure tubes act as channels of heat transfer in the pressurized water type of nuclear reactors and contain the fuel bundles. These tubes are subjected to high pressure, moderate temperature and high fluence of neutrons during the reactor operation. During service, the mechanical and fracture properties of these tubes degrade due to various material ageing phenomena including those of irradiation. In order to have better mechanical and corrosion properties in the irradiated water environment and to ensure minimum absorption cross-section for neutrons, Zirconium based alloys are usually used for manufacturing of these tubes [1-2]. The manufacturing route of these pressure tubes from the ingots is also complicated with several stages of mechanical working and heat-treatment procedures. For example, the pressure tubes of current Indian pressurized heavy water reactors (PHWRs) are manufactured from quadruple-melted ingots of Zr-2.5Nb alloys [3]. Similarly, the fuel-clad tubes are also manufactured from different types of Zirconium alloys through a series of mechanical working and heat-treatment processes. Due to the long term exposure to aggressive environments in the reactor, significant degradation in properties of the fuel-clad tubes has also been reported by various researchers in the literature [4-8].

For design and safety analysis of the pressure tubes as well as of the fuel-clad tubes, it is essential to evaluate the mechanical properties in the as-manufactured as well as in the in-service conditions. Due to the complex mechanical working and heat-treatment conditions experienced by these tubes during their manufacture, the mechanical properties of the pressure tubes are highly anisotropic. It is not possible to

evaluate the transverse mechanical properties from the standard tensile tests as standard specimens with sufficient dimensions cannot be machined from the pressure tubes in the circumferential direction (the radius of curvature is too small for this purpose). Similar problem is also faced by the engineers in the mechanical property evaluation of fuel-clad tubes [9-23]. Several types of geometry of specimens and the loading-mandrels were designed by various researchers world-over in order to determine the mechanical and fracture properties of these tubes satisfactorily.

A pin-loading tension (PLT) test was designed by Grigoriev et al. [20] to evaluate the fracture toughness of Zicaloy-2 fuel claddings. Axially notched ring specimens cut from the fuel cladding section have been tested in a way similar to that used to test compact-tension specimens. Hsu et al. [21] have designed an X-shaped specimen and have used it to determine the fracture toughness of the thin-walled tubular materials. In this method, two curved axially-cracked semi-cylindrical specimens (machined from the fuel-clad tubes) were glued together by epoxy adhesive to make an X-shaped specimen so as to minimize the bending effects of the loading. A modified ring tension test was carried out by Jossefson and Grigoriev [22] for fracture toughness testing of cladding where flattening of the ring is prevented by means of a central piece which is inserted into the ring. The central piece has almost the same dimension as that of the ring's internal diameter. An internal conical mandrel technique has been used in Ref. [23] for evaluation of fracture toughness of fuel-clad tubes.

In the recent years, specimens have been machined from the fuel-clad tubes in the form of rings of small width and tested with special types of loading mandrels. In this work, a similar technique is followed for the specimens machined from the pressure tubes, which has not received much attention in literature. However, the results from these tests cannot be used directly to evaluate the material stress-strain curve. The complexities lie in (a) existence of both tensile and bending stresses in the loading cross-section due to the curvature of the specimen, (b) effect of lateral pressure and friction drag exerted by loading mandrels on the specimen, (c) geometry of the loading mandrel and the initial gap between the mandrels, (d) orientation of gauge-length of reduced cross-section of the ring-specimen with respect to the loading axis and so on.

The aim of this work is to investigate the effects of the above-mentioned factors on the load-deformation response of the ring-tension test setup with a detailed 3-D finite element (FE) analysis and develop a suitable inverse FE analysis procedure so that the mechanical properties in the transverse direction of the pressure tubes can be satisfactorily evaluated from the test data. The mechanical properties in the axial direction of the pressure tubes can also be determined from the inverse FE analysis of tensile test data obtained from testing of straight specimens machined from the axial direction of these tubes.

In this work, experiments have been conducted on the ring-type specimens machined from the pressure tubes of two different types of materials loaded with different types of mandrels and the results of load-deformation response have been compared with those of FE simulation. It can be concluded that the finite element analysis procedure of this complex loading setup should be used to evaluate the accurate transverse mechanical properties in terms of the material true stress-strain curve.

This paper is divided into five sections. A brief description of the materials used in this work, design of the ring specimen and the test setup is provided in Section-2. The details of the finite element analysis procedure used in this work for simulation of deformation behavior of the test setup are given in Section-3. The results from FE analysis have been compared with those of experiments and the implications of FE analysis have been discussed in Section-4 followed by conclusions and scope of future research in Section-5.

BRIEF DESCRIPTION OF THE MATERIAL, SPECIMEN AND THE RING-TENSION TEST-SETUP

In this work, specimens in the form of circular rings have been machined from both Zircaloy-2 as well as Zr-2.5%Nb pressure tubes. Both of these materials have been used in the manufacture of pressure tubes of Indian PHWRs. Zircaloy-2 have been used in older type of PHWRs whereas Zr-2.5%Nb is used now-a-days due to the important property of lower hydrogen pick-up of these alloys from the flowing coolant (i.e., heavy water) inside the pressure tubes. The chemical composition of both of these alloys is given in Table-1 and 2 respectively. It can be noted that Zr-2.5Nb alloys contains 2.58 wt. % of Nb in addition to other alloying elements. However, the wt. % of Cr and Ni are significantly lower in comparison to those of Zircaloy-2. The major alloying elements in Zr-2.5Nb pressure tubes are niobium and oxygen. Niobium is a beta stabilizer and the presence of the same in the alloys leads to the formation of a two-phase microstructure consisting of hcp α and bcc β phases. The presence of niobium in zirconium is known to increase the tensile and creep-strength of the alloy significantly. Hence, Zr-Nb alloys show improved creep resistance as compared to the other Zirconium alloys (e.g., Zircaloy-2). This is also one of the considerations for using Zr-2.5Nb alloy instead of Zircaloy-2 as the pressure tube material in the current Indian PHWRs.

Table-1: Chemical composition of Zircaloy-2 pressure tube material

Element	Sn	Fe	Cr	Ni	O	Zr
Wt. %	1.5	0.09	0.1	0.05	0.12	rest

Table -2 Chemical composition of Zr-2.5Nb pressure tube material

Element	Al	C	P	N	O	Fe	Ni	Cr	Nb	Si	Sn	Zr
Wt. %	0.003	0.01	0.001	0.0026	0.11	0.13	0.004	0.017	2.58	0.003	0.0056	rest

(a) (b)

Fig. 1: (a) Ring-tension specimens with a gauge-length of reduced cross-section machined from Indian PHWR pressure tubes and tested to failure in the ring-tension setup; (b) Solid model of the ring-tension specimen, the symmetric form of which was used in FE analysis

The fabrication of these pressure tubes consists of four major steps, viz., hot extrusion, two cold-pilgering stages with an intermediate annealing step (at 550 deg. C for 6 hours) and a final autoclaving stage (in 10 bar steam atmosphere at 400 deg. C for 36 hours). These mechanical working conditions also affect the texture of this material which is expressed in terms of Kearns' factor 'f'. The preferential orientation (in terms of Kearns' factor) of basal poles (i.e., the <c> directions) along transverse, radial and longitudinal

directions are of the order of 0.58, 0.39 and 0.03 respectively [3]. Hence, the mechanical properties of these tubes are highly anisotropic.

The ring-tensile specimens have been machined from the as-manufactured tubes and tested in a ring-tension setup. The pictures of the tested specimen are shown in Fig. 1(a). The 3-D solid model of the specimen used in the FE analysis is shown in Fig. 1(b). The rings machined from the Zircaloy-2 pressure tube have internal diameter values of 83 mm and the value of thickness as 4.3 mm, whereas for the rings machined from Zr-2.5Nb pressure tubes, the corresponding dimensions are 83 mm and 3.6 mm respectively. A section of the ring specimen has a reduced cross-section (known as gauge-length section) in order to induce necking in the same region. The width of both of the ring specimens is 6 mm in the gauge-length section and 12.5 mm away from the gauge-length section. The specimen having a single reduced gauge-length in the periphery is also known as the single-gauge-length (SGL) specimen. The gauge length has a dimension of 25 mm in case of the Zircaloy-2 ring-specimen, whereas it is of 20 mm in case of the Zr-2.5Nb ring-specimen. The gague-length can be oriented at different angles with respect to the loading axis of the testing machine. When the gauge-length is oriented at right angle to the loading axis, the arrangement is known as "12 'O' clock position" in this paper.

The ring-tension setup consists of the ring-specimen and the loading mandrel. The loading mandrel can be of various designs. We have considered two types of loading mandrels (i.e., 2-piece and 3-piece type of mandrel) in this work. The 2-piece mandrel consists of two semi-cylindrical mandrels with a gap between them and they load against the ring-specimen with the help of loading pins. In case of the 3-piece mandrel, a central piece is inserted in between the top and the bottom loading mandrels in order to restraint the lateral movement of the ring-specimen during loading. The loading arrangements with the 2-piece and 3-piece mandrels are shown in Fig. 2(a-c) respectively.

(a) (b) (c)

Fig. 2: Ring specimen with gage-length oriented at 12'O clock position in the test grips. (a) 2-piece mandrel, pins and the loading grip before assembling the parts; (b) 2-piece mandrels fitted with ring specimen loaded in the grips; (3) 3-piece mandrels fitted with ring specimen loaded in the grips

FINITE ELEMENT ANALYSIS OF RING-TENSION SETUP

A 3-D finite element model of the ring-tension setup has been prepared. Keeping in mind of the symmetric boundary conditions, only one-half of the test-setup has been modeled as shown in Fig. 3(a) and 3(b) for the 2-piece and 3-piece type of loading mandrels respectively. The FE mesh uses 3-D 20-

noded iso-parametric brick elements with tri-quadratic interpolation functions for the nodal variables (i.e., displacements in three Cartesian co-ordinate directions). The von Mises yield condition along with the Prandtl-Reuss flow rule have been used as the constitutive model for the elastic-plastic FE analysis.

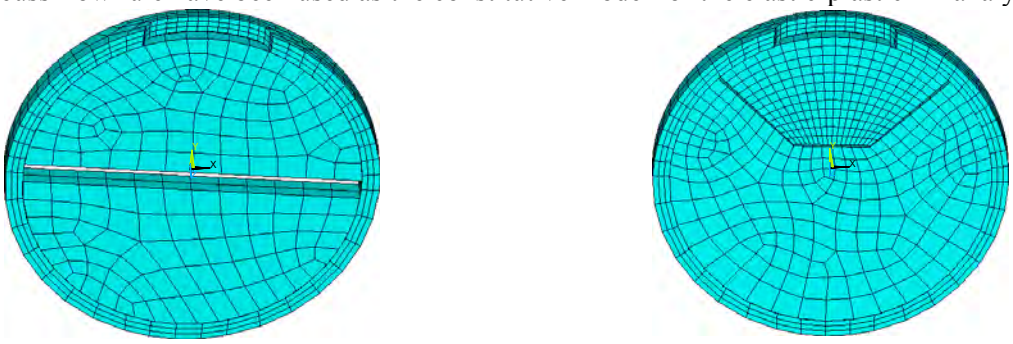

(a) (b)

Fig. 3: FE mesh of the ring-tension setup. SGL specimen with (a) 2-piece loading mandrel, (b) 3-piece loading mandrel. 3-D elements for both specimen and mandrel with contact elements at the interface have been used in the analysis

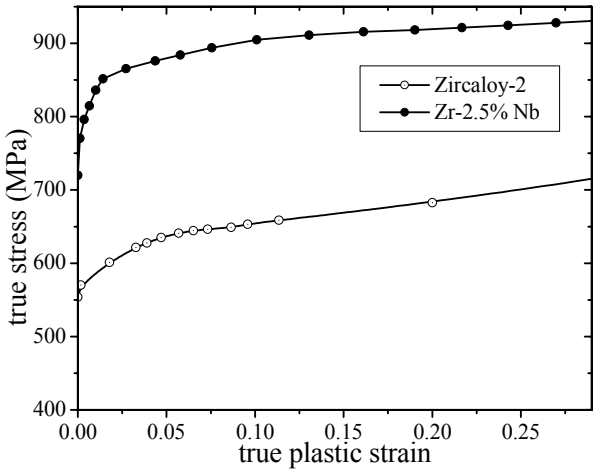

Fig. 4: True stress-strain curves of pressure tube material of Indian PHWR (Zircaloy-2 and Zr2.5%Nb)

The mandrels are in contact with the ring-specimen during loading and hence, surface-to-surface contact elements between the loading mandrels and the specimen have been used in the analysis. In the experiment, Teflon tapes are introduced between the mandrels and the specimen in order to reduce the co-efficient of friction between the contacting surfaces. A friction co-efficient value of 0.02 has been used in this FE analysis which is typical for the sliding condition existing between Teflon and the metallic materials. The mandrel is made up of SS403 stainless steel. The Young's modulus and Poisson's ratio for the mandrel material at room temperature has been taken as 210 GPa and 0.3 respectively. The Young's modulus and Poisson's ratio for the pressure tube materials at room temperature have been taken as 92 GPa and 0.35 respectively in this FE analysis. The results of FE analysis in terms of load-deformation response of the ring-tension setup have been compared with those of experiment and the details are presented in the next section.

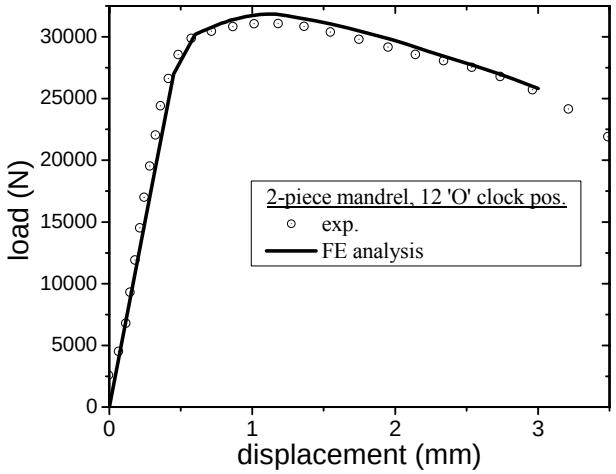

Fig. 5: Load-displacement response of the Zircaloy-2 ring-tension specimen with 2-piece loading mandrel and gauge-length oriented perpendicular to loading axis (exp vs. FE analysis)

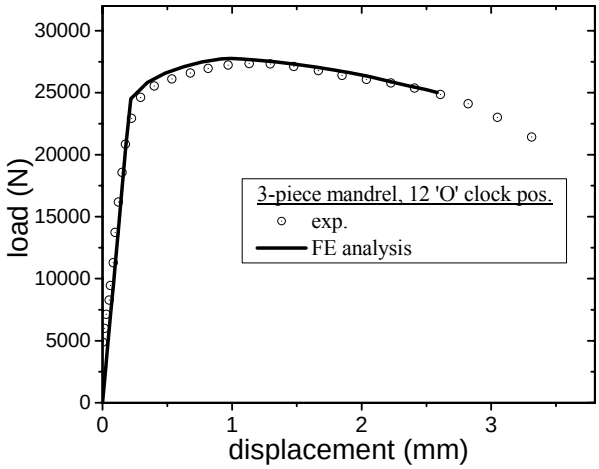

Fig. 6: Load-displacement response of the Zircaloy-2 ring-tension specimen with 3-piece loading mandrel and gauge-length oriented perpendicular to loading axis (exp vs. FE analysis)

RESULTS AND DISCUSSION

The objective of this work has been to study the effect of geometrical design of the loading mandrels and the contact condition between the mandrels and the ring-specimen on the load-deformation behavior of the test setup. For this purpose, two types of loading mandrels have been considered in the experiment and their subsequent FE analysis. Two types of Zirconium alloys having significantly different mechanical properties have been considered in this work. The purpose is to test the validity of this approach for materials with widely varying stress-strain behavior. The material true stress-strain curve (in terms of true stress vs. true plastic strain) is required for FE analysis of the test setup. As the ring-tension tests are done at room temperature, the above data is required for the materials at room temperature and the same are shown in Fig. 4 for Zircaloy-2 and Zr-2.5%Nb respectively.

The yield stress (YS) and ultimate tensile strength (UTS) values of Zircaloy-2 are given as 554 MPa and 605.8 MPa respectively. The values of the above parameters are 720 MPa and 842 MPa respectively for the material Zr-2.5%Nb. It may be noted from Fig. 4 that Zr-2.5%Nb exhibits significant plastic strain hardening before the strength level reaches UTS compared to Zircaloy-2. However, plastic strain value at UTS for Zr-2.5%Nb is significantly lower (i.e., 0.028) compared to that of Zircaloy-2 (i.e., 0.047) which indicates that Zr-2.5%Nb has a lower uniform ductility compared to that of Zircaloy-2. In the post-necking region of deformation, the plastic strain hardening behavior of Zr-2.5%Nb is lower compared to that of Zircaloy-2 as can be seen from the slopes of the material stress-strain curves (beyond the UTS region) in Fig. 4. The material stress-strain curves as depicted in Fig. 4 have been used in the FE analysis as an input. The load-displacement curve of test setup can be determined from FE analysis using the procedure as discussed below.

In the FE analysis, the lower mandrel has been fixed whereas the upper mandrel has been provided with incremental displacements in several displacement-controlled loading steps. The reaction values at the loading nodes of the mandrel have been summed up in order to calculate the total load. This value of load along with the applied displacement at any nodal point (among the loading nodes) has been plotted at different steps in order to represent the load-displacement response of the test set-up. The experiment load-displacement data as directly collected from the machine needs to be corrected for the effect of machine compliance. For this purpose, a blank ring-specimen (without the reduced cross-section gauge length) has been tested and the machine compliance has been determined from the above data. The

original load-displacement data as obtained from the testing of SGL ring-specimens have been corrected by taking into account of the machine compliance as determined from the above procedure. The load-displacement response of the test-setup with 2-piece loading mandrel and the Zircaloy-2 ring (with the gauge length oriented at 12 'O' clock position) as obtained from FE analysis has been plotted in Fig. 5 along with the experimental load-displacement data.

It may be noted that FE analysis has been able to correctly predict the experimental yield load, maximum load as well as the post-necking behavior very accurately. The load-deformation behavior in a problem with contact type of boundary conditions can be quite complex due to making and breaking of contact at the interfaces of the loading mandrel and the ring-specimen. As the outside curvature of the loading mandrel (with the Teflon tape on it) is nearly same as that of the inside curvature of the ring specimen, there is a surface-to-surface contact of nearly 180 degree angle (in case of 2-piece type of loading mandrel) at the beginning of loading. The gauge-length portion of the ring specimen rests on the mandrel and is subjected to extension in the circumferential direction due to relative movement of the two mandrels. The extension in the gauge-length section of ring specimen develops due to the indirect loading conditions because of the contact constraint of the mandrels exhibited with respect to the ring specimen. Once the gauge-length section starts to deform uniformly, there will be alteration in the contact conditions. However, significant effect of the change in contact conditions between the mandrel and the gauge-length section can be observed once necking sets in.

The necking of the gauge-length results in significant reduction in cross-section and the interface contact condition breaks and the necked-region now starts deforming independently. However, the contact condition still prevails in the other regions of ring-specimen away from the necked-region in both sides of the loading axis. Till necking, the mandrel exerts a lateral pressure as well as a friction drag on the lower contact surface of the ring cross-section (in the gauge-length region) and this will have significant effect on yield behavior of the specimen. It may be noted that the direction of lateral pressure is normal to the contact surface and hence, it is parallel to the loading direction, whereas the friction drag has two different directions on both sides of the loading axis as the direction of relative motion between the loading mandrel and the ring-specimen changes. The specimen gauge-length tries to move to the left hand side relative to the mandrel in the left hand side of the loading axis, whereas the motion is exactly opposite in the right hand side of the loading axis.

As the values of friction drag as well as lateral pressure depend nonlinearly on the displacement of the loading mandrel, these are very difficult to estimate in a closed form solution of the elastic-plastic deformation behavior of the test setup. However, the FE analysis used in this work has been very well able to simulate the accurate contact conditions and hence, the resulting load-displacement curve for the whole displacement range compare very well with that of experiment as shown in Fig. 5. The FE analysis has then been carried out for the test-setup with 3-piece loading mandrel. The gauge-length of the SGL ring-specimen is also aligned in 12 'O' clock position in this experiment. The load-displacement result of FE analysis of the test-setup with 3-piece mandrel has also been compared with that of experiment in Fig. 6 and the FE result is very close to that of experiment in the whole range of deformation.

It can be observed that the maximum load as obtained from the two tests (with identical specimen, however with different designs of loading mandrels, i.e., 2-piece vs. 3-piece) are quite different (Fig. 5 vs. Fig. 6). The test with the 2-piece mandrel shows a higher maximum load (at onset of necking) compared to that of the test with 3-piece mandrel. This is because of the effect of contact conditions existing at the interface of the mandrel and the ring-specimen as discussed earlier. The contact pressure and surface traction for the 2-piece mandrel are active over a region with approximately 180 degree angle, whereas for the 3-piece mandrel, the same is around 90 degree. This is because of geometry of the loading mandrel. Hence, the resulting load for a given displacement is lower for the test with 3-piece mandrel compared to that of the 2-piece mandrel. If one determines the engineering strain-strain curve from the experimental load-displacement curve directly (using standard equations of tensile tests), the results will be very different for the two tests though the material and the specimen geometry are same. This is

because the effect of friction and contact boundary conditions existing at the interface of the specimen and the loading mandrel are not taken into account in the calculation of engineering stress and engineering strain in the standard equations. It is also not possible to introduce the above effects in a closed form equation because of the complexities involved as discussed earlier. Hence, a 3D FE analysis with capability to handle the above effects is essential for accurate estimation of material stress-strain curve through an inverse analysis procedure.

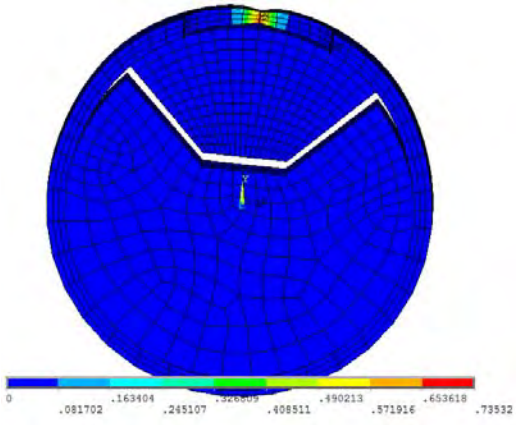

Fig. 7: von Mises equivalent plastic strain contour in the Zr2.5%Nb ring-tensile specimen loaded with 3-piece mandrel for an applied displacement of 3 mm

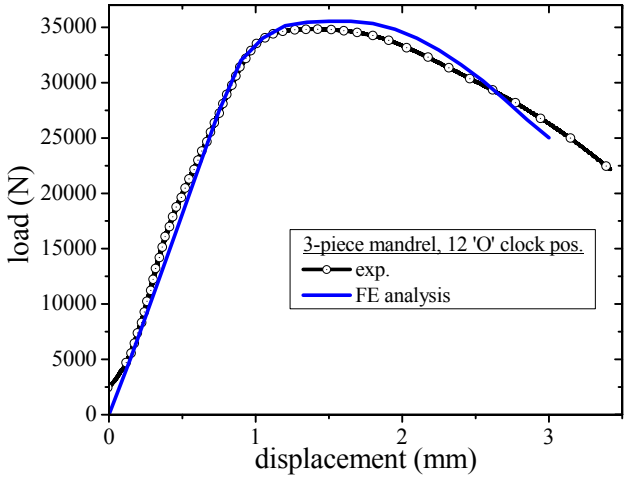

Fig. 8: Load-displacement response of the Zr2.5%Nb ring-tension specimen with 3-piece loading mandrel and gauge-length oriented perpendicular to loading axis (exp vs. FE analysis)

It may be noted that the FE analysis is able to successfully predict the different values of maximum load as well as the post-necking behavior of the two test-setups with a single data of material stress-strain curve as the input. Hence, the inverse FE analysis is able to estimate the same material stress-strain curve from the two different types of tests albeit prediction of completely different load-displacement responses and hence, it acts as a true transfer function between the material response (dependent only upon material property and independent of geometry of specimen and loading mandrel) and the system response. The calculation procedure of engineering stress and strain is also not straight forward as the deformation in a ring is similar to deformation in a statically indeterminate system. This is because of redistribution of load and deformation along the circumference of the ring during loading as the ring is continuous. For this purpose, the engineering stress at the gauge section of the ring is calculated by dividing the half of the total load (as the load is shared equally between the two diametrically-opposite cross-sections of the ring, though these are of different values of cross-sectional area) by the area of cross-section of the gauge section (i.e., with reduced value). Similarly, the engineering strain is calculated by dividing the twice of the displacement magnitude of the loading mandrel (the two vertical legs of the ring being deformed simultaneously due to the relative movement of the mandrels) with the gauge length of the ring-specimen.

In order to validate the above procedure for another type of pressure tube alloy (i.e., Zr2.5%Nb), tests have been conducted on a ring specimen with a 3-piece loading mandrel. The dimensions of the ring-specimen machined from Zr2.5%Nb pressure tube of Indian PHWR have been provided in Section-2. The material true stress-strain curve used as input data for this material in the FE analysis is shown in Fig. 4. The values of co-efficient of friction and other parameters used in the contact analysis of this specimen are exactly same as that used in the previous FE analysis with Zircaloy-2 ring specimens. The deformed shape of the ring-specimen along with the von Mises equivalent plastic strain contour is shown in Fig. 7 for a displacement value of 3 mm applied on the loading mandrel. It may be noted that the specimen has undergone significant necking at this value of applied mandrel displacement and the actual value of local

von Mises equivalent plastic strain is 73.5% approximately (Fig. 7). However, the engineering strain as calculated from the applied displacement (2x3 mm) and the gauge length (20 mm) is around 30%. This is because of the presence of multi-axial deformation and hence, a multi-axial state of stress in the necked-region. The calculation of engineering strain (as 30%) is valid for a pure uni-axial deformation case.

Fig. 7 also shows that the contact between the middle loading mandrel and the specimen breaks on both sides of loading axis and hence, the contact conditions are significantly different in comparison to that of a 2-piece mandrel where the contact remain intact in approximately 180 degree angle of the loading mandrel throughout the deformation history (except the portion of necked-region after necking has started). The load-displacement response of the test-setup with 3-piece mandrel and the Zr2.5%Nb ring-specimen as been determined from FE analysis has been compared with that of experiment in Fig. 8. It may be noted that the FE analysis has also been able to satisfactorily predict the experimental load-displacement behavior of this test-setup for a different alloy. Hence, the procedure is validated and this gives confidence in the use of this combined FE analysis and experimental procedure for accurate estimation of transverse mechanical properties of the Zircaloy pressure tubes in the as-manufactured as well as in the service-exposed conditions, which is very crucial for the design as well as safety analysis of these components.

CONCLUSIONS

Use of ring-specimens for evaluation of mechanical properties in the as-received as well as service-exposed conditions of nuclear reactor pressure tubes is very attractive due to the ease of machining of the specimens and testing in different conditions including those of irradiation. However, the mechanical properties cannot be directly evaluated due to complexity of the test-setup. In this work, a 3-D FE analysis procedure has been adopted and it was shown that it is possible to estimate the load-displacement response of the test-setups accurately by taking into account of the variability in mandrel design and contact conditions. The dynamic nature of evolution of contact conditions during loading and hence, the effect of additional stresses (i.e., those due to lateral pressure and interface drag) on the yield and subsequent material strain-hardening behavior cannot be taken care of in standard empirical equations as used for uni-axial tensile tests. Hence, use of a 3-D FE analysis (as used in this work) is recommended for accurate estimation of material properties from these ring-tension tests. The scope of future work includes assessment of the above procedure for other engineering materials such as low-alloy steels and for other tubular components used in different engineering applications.

REFERENCES

1. Nikulina, A.V. Zirconium-Niobium Alloys for Core Elements of Pressurized Water Reactors. Metal Science and Heat Treatment 2003; 45(7-8): 287-292.
2. Nikulina, AV. Zirconium alloys in nuclear power engineering. Metal Science and Heat Treatment 2004; 46(11-12): 458-462.
3. V. Deshmukh, U. Singha, S. Tonpe, N. Saibaba. Effect of process variables on texture and creep of pressurized heavy water reactor pressure tubes. Transactions of the Indian Institute of Metals 2010; 63(2-3): 397-402.
4. Edsinger, K., Davies, J.H., and Adamson, R.B. Degraded fuel cladding fractography and fracture behaviour. Ziconium in nuclear industry: 12th International symposium, ASTM STP 1354. G.P. Sabol and G.D. Moan, Eds., Americal Society for Testing and Materials, West Conshohocken, PA, 2000, 316-339.
5. Murty K. L. Deformation, texture and microstructure- property correlation and in-reactor performance of of Zircaloy cladding in LWRs. Proceedings of the international symposium on Advances in Zirconium-2002, September 11-13, Mumbai, India, 2002, 28-45.

6. Murty, K. L. Texture based physical, mechanical and corrosion characteristics of Zirconium alloys. Textures in Materials Research, Oxford and IBH co. Ltd, New Delhi, 1999, 113-126.
7. Wang, Y. and Murty, K. L. Effect of temperature on mechanical anisotropy of re-crystallized Zircaloy-4 sheet. Proc. 4th Asia-Pacific symposium on Advances in Engineering plasticity and its applications, AEPA 98, Seoul, South Korea, 21-25 June 1998.
8. Leclercq S., Parrot A., and Leroy M. Failure characteristics of cladding tubes under RIA conditions. Nuclear Engineering and Design 2008; 238(9): 2206–2218.
9. Arsene, S., and Bai, J. A New Approach to measuring transverse properties of structural tubing by a ring test. J. Testing Evaluation 1996; 24(6): 386-391.
10. Bae, B.-K., Cho, S.-K., Seok, C.-S. A study on ring tensile specimens. Materials Science and Engineering 2008; A483-484: 248-250.
11. Seok, C.S., Bae, B.K., Koo, J.M., Murty, K.L. The properties of the ring and burst creep of ZIRLO cladding. Engineering Failure Analysis 2006; 13: 389-97.
12. Lee,K.W., Hong, S.I. Zirconium hydrides and their effect on the circumferential mechanical properties of Zr-Sn-Fe-Nb tubes. Journal of Alloys and Compounds 2002; 346: 302-307.
13. Bertolino, G., Meyer, G., and Perez, I.J. In-situ crack growth observation and fracture toughness measurement of hydrogen charged zircaloy-4. J. Nucl. Mater. 2003; 322: 57-65.
14. Fukuda, T., Itagaki, N., Kamimura, J., Mozumi, Y. and Furuya, T. Fracture toughness of hydrogen-absorbed zircaloy-2 cladding tube. European Nuclear Society, Topfuel 2003, Wurzburg, Germany, 16-19 March 2003.
15. Videm, K. and Lunde, L. Stress corrosion cracking and growth formation of pellet-clad interaction defects. Ziconium in nuclear industry: 4th International symposium, ASTM STP 681. J.H. Schemel and T.P. Papazoglou, Eds, Americal Society for Testing and Materials, West Conshohocken, PA, 1979, 230-237.
16. Lee, K.W., Kim, S.K., Kim, K.T., Hong, S.I. Ductility and strain rate sensitivity of Zircaloy-4 nuclear fuel claddings. Journal of Nuclear Materials 2001; 295: 21-26.
17. Grigoriev, V., Josefsson, B. Rosborg, B. and Bai, J. A novel fracture toughness testing method for irradiated tubing-experimental results and 3D numerical evaluation. Transactions of the 14th Int. Conference on Structural Mechanics in Reactor Technology, Lyon, France, 1997, 57-64.
18. Nakatsuka, M., Kubo, T. and Hayashi, Y. Fatigue Behavior of Neutron Irradiated Zircaloy-2 Fuel Cladding Tubes. Ziconium in the Nuclear Industry: Ninth International Symposium, ASTM STP 1132, C.M. Eucken and A.M. Garde Eds., American Society for Testing and Materials, 1991, 230-245.
19. Yoshitake T., Abe Y., Akasaka N., Ohtsuka S., Ukai S. and Kimura A. Ring-tensile properties of irradiated oxide dispersion strengthened ferritic/martensitic steel claddings. Journal of Nuclear Materials 2004; 329-333: 342–346.
20. Grigoriev, V., Josefsson, B., Lind, A. and Rosborg, B. A pin-loading tension test for evaluation of thin-walled tubular materials. Scripta Metallurgica et Materialia 1995; 33(1): 109-114.
21. Hsu, H.H., Chien, K.F., Chu, H.C., and Liaw P.K. An X-specimen test for determination of thin walled tube fracture toughness. Fatigue and Fracture Mechanics: 32nd Volume, ASTM STP 1406, R. Chona, Ed.. Americal Society for Testing and Materials, West Conshohocken, PA, 2001, 214-226.
22. Josefsson, B., and Grigoriev, V. Modified Ring Tensile Testing and a New Method for Fracture Toughness Testing of Irradiated Cladding. Studsvik Material AB, S-61182, Nykoping, Sweden, May 22, 1996.
23. Sainte Catherine, C., Le Boulch, D., Carassou, S., Ramasubramanian, N. And Lemaignan, C. An internal conical mandrel technique for fracture toughness measurements on nuclear fuel cladding. ASTM J. of Testing and Evaluation 2006; 34(5): 373-382.